Inorg. Chem. **2008**, *47*, 863–874

Conducting Dimerized Cobalt Complexes with Tetrathiafulvalene Dithiolate Ligands

Emiko Fujiwara,[†] Kazumasa Hosoya,[†] Akiko Kobayashi,*[,†,‡] Hisashi Tanaka,[§] Madoka Tokumoto,[§] Yoshinori Okano,[||] Hideki Fujiwara,[||] Hayao Kobayashi,[‡,||] Yuichi Fujishiro,[⊥] Eiji Nishibori,[⊥] Masaki Takata,[#] and Makoto Sakata[⊥]

Research Centre for Spectrochemistry, Graduate School of Science, The University of Tokyo, Hongo, Bunkyo-ku, Tokyo 113-0033, Japan, Department of Chemistry, College of Humanities and Sciences, Nihon University, Sakurajosui, Setagaya-ku, Tokyo 156-8550, Japan, Nanotechnology Research Institute, National Institute of Advanced Industrial Science and Technology, Umezono 1-1-1, Tsukuba 305-8568, Japan, Institute for Molecular Science and CREST, JST, Myodaiji, Okazaki 444-8585, Japan, Department of Applied Physics, Nagoya University, Nagoya 464-8603, Japan, and RIKEN SPring-8 Center and CREST, JST, 1-1-1, Kouto, Sayo-cho, Sayo-gun, Hyogo 679-5148, Japan

Received June 5, 2007

To obtain novel single-component molecular metals, we attempted to synthesize several cobalt complexes coordinated by TTF (tetrathiafulvalene)-type dithiolate ligands. We succeeded in the syntheses and structure determinations of $(^n\mathrm{Bu}_4\mathrm{N})_2[\mathrm{Co(chdt)}_2]_2$ (**1**), $(^n\mathrm{Bu}_4\mathrm{N})_2[\mathrm{Co(dmdt)}_2]_2$ (**2**), $[\mathrm{Co(dmdt)}_2]_2$ (**3**), and $[\mathrm{Co(dt)}_2]_2$ (**4**) (chdt = cyclohexeno-TTF-dithiolate, dmdt = dimethyl-TTF-dithiolate, and dt = TTF-dithiolate). Structure analyses of complexes **1**–**4** revealed that two monomeric $[\mathrm{Co(ligand)}_2]^-$ or $[\mathrm{Co(ligand)}_2]^0$ units are connected by two Co–S bonds resulting in dimeric $[\mathrm{Co(ligand)}_2]_2^{2-}$ or $[\mathrm{Co(ligand)}_2]_2$ molecules. Complex **1** has a cation–anion-intermingled structure and exhibited Curie–Weiss magnetic behavior with a large Curie constant (C = 2.02 K·emu·mol^{-1}) and weak antiferromagnetic interactions (θ = –8.3 K). Complex **2** also has a cation–anion-intermingled structure. However, the dimeric molecules are completely isolated by cations. Complexes **3** and **4** are single-component molecular crystals. The molecules of complex **3** form two-dimensional molecular stacking layers and exhibit a room-temperature conductivity of σ_{rt} = 1.2 × 10^{-2} S·cm^{-1} and an activation energy of E_a = 85 meV. The magnetic behavior is almost consistent with Curie–Weiss law, where the Curie constant and Weiss temperature are 8.7 × 10^{-2} K·emu·mol^{-1} and –0.85 K, respectively. Complex **4** has a rare chair form of the dimeric structure. The electrical conductivity was fairly large (σ_{rt} = 19 S·cm^{-1}), and its temperature dependence was very small ($\sigma_{0.55K}/\sigma_{rt}$ = ca. 1:10), although the measurements were performed on the compressed pellet sample. Complex **4** showed an almost constant paramagnetic susceptibility ($\chi_{300\ K}$ = 3.5 × 10^{-4} emu·mol^{-1}) from 300 to 50 K. The band structure calculation of complex **4** suggested the metallic nature of the system. Complex **4** is a novel single-component molecular conductor with a dimeric molecular structure and essentially metallic properties down to very low temperatures.

Introduction

Over the past few decades, almost all molecular metals and superconductors have been realized by charge-transfer phenomena which generate charge carriers; in other words, more than two chemical species are required for the formation of molecular conductors.[1,2] Until recently, all the molecular crystals comprising single-component molecules were believed to be insulators because they comprise closed-

* To whom correspondence should be addressed. E-mail: akoba@chs.nihon-u.ac.jp.
[†] The University of Tokyo.
[‡] Nihon University.
[§] National Institute of Advanced Industrial Science and Technology.
[||] Institute for Molecular Science and CREST, JST.
[⊥] Nagoya University.
[#] RIKEN SPring-8 Center and CREST, JST.

(1) Williams, J. M.; Ferraro, J. R.; Thorn, R. J.; Carlson, K. D.; Geiser, U.; Wang, H. H.; Kini, A. M.; Whangbo, M.-H. *Organic Superconductors (Including Fullerenes)*; Prentice Hall: Upper Saddle River, NJ, 1992.
(2) Ishiguro, T.; Yamaji, K.; Saito, G. *Organic Superconductors*, 2nd ed.; Springer-Verlag: Berlin, Heidelberg, 1998.

10.1021/ic701100r CCC: $40.75
Published on Web 01/08/2008

shell molecules connected by a weak intermolecular van der Waals force and have no charge carriers in the crystals. On the other hand, in the case of typical inorganic metals such as sodium and copper, free electrons are automatically generated when each neutral element is self-assembled by metal bonds. In comparison with these inorganic metals, the conducting electrons of single-component molecular conductors tend to be localized by an electron correlation effect, even when electronic bands are formed by aggregation. Consequently, the spontaneous generation of free carriers appears to be extremely difficult in these systems. However, since the mid-1990s, single-component transition-metal complexes with tetrathiafulvalene (TTF) frameworks have been reported to be conductive to some extent.[3−8] We noticed that free carriers can be generated even in single-component molecular crystals when the molecule has an unprecedented small HOMO (highest occupied molecular orbital)−LUMO (lowest unoccupied molecular orbital) gap and large intermolecular transverse interactions.[9,10] Several years ago, the first example of a single-component molecular metal was synthesized on the basis of the transition-metal complex molecule with extended TTF ligands, [Ni(tmdt)$_2$] (tmdt = trimethylene-TTF-dithiolate), which retained a metallic state down to 0.6 K.[10−12] Rigorous experimental evidence for the existence of a Fermi surface in this single-component molecular crystal was obtained by detecting the quantum oscillations in magnetization at a very high magnetic field and a very low temperature (or de Haas-van Alphen (dHvA) effect), showing the presence of three-dimensional (3D) electron and hole Fermi surfaces in [Ni(tmdt)$_2$].[13,14]

An isostructural gold complex [Au(tmdt)$_2$] was also prepared.[15] The room-temperature conductivity (σ_{rt}) measured on the compressed pellet sample was found to be 50 S·cm^{-1}.[16] The recent resistivity measurements on a polycrystalline sample by H. Tanaka et al. showed that it retained its metallic conductivity down to 4 K.[17] The electronic structure of [Au(tmdt)$_2$] is completely different from that of [Ni(tmdt)$_2$] because the neutral bis(dithiolato)gold complex has an odd number of total electrons. In fact, [Au(tmdt)$_2$] underwent an antiferromagnetic transition at around 110 K without loss of its metallic conductivity.[16] Magnetic susceptibility measurements and the first principle band structure calculation suggested that the Fermi surface of [Au(tmdt)$_2$] remains below 110 K, which retains the metallic nature of the system even below the antiferromagnetic transition temperature.[18] [Au(tmdt)$_2$] is the first molecular metal wherein the magnetic order and conduction electrons coexist at temperatures higher than 100 K.

After the achievement of the first single-component molecular metal, one of the next targets was a single-component magnetic molecular metal with localized magnetic moments on the central transition-metal atom. We developed [Cu(dmdt)$_2$] (dmdt = dimethyl-TTF-dithiolate).[19] The central copper atom has a tetrahedral coordination, and the dmdt ligands take on an arrangement similar to the donor array in "κ-type organic superconductors."[20] In addition, [Cu(dmdt)$_2$] exhibited Curie−Weiss behavior, which suggested the existence of 84% of $S = {}^1/_2$ magnetic moments.[19]

Recently, we have also examined cobalt complexes because the cobalt(II) atom can have a magnetic moment larger than that of the copper(II) atom. We focused on the TTF-type ligands fused with a six-membered ring such as a cyclohexeno ring because six-membered rings have greater structural flexibility as compared with the structurally rigid five-membered rings and show the possibility of possessing unique and variable structural modifications and the resultant novel electronic properties.[21] Besides, we used methyl-substituted and unsubstituted TTF-dithiolate ligands because they are expected to form a tightly packed structure of the neutral metal complexes in the solid state. In this Article, we report the syntheses, structures, and physical properties of novel cobalt complexes with TTF-dithiolate ligands, (^{n}Bu$_4$N)$_2$[Co(chdt)$_2$]$_2$ (**1**) (chdt = cyclohexeno-TTF-dithiolate), (^{n}Bu$_4$N)$_2$[Co(dmdt)$_2$]$_2$ (**2**), [Co(dmdt)$_2$]$_2$ (**3**), and [Co(dt)$_2$]$_2$ (**4**) (dt = TTF-dithiolate), whose complexes exhibit a unique dimerized structure connected by two single bonds between the sulfur and cobalt atoms of two [Co(ligand)$_2$] units[22] (Chart 1). The crystal structure determination of [Co-

(3) Narvor, N. L.; Robertson, N.; Weyland, T.; Kilburn, J. D.; Underhill, A. E.; Webster, M.; Svenstrup, N.; Becher, J. *Chem. Commun*. **1996**, 1363−1364.
(4) Narvor, N. L.; Robertson, N.; Wallace, E.; Kilburn, J. D.; Underhill, A. E.; Bartlett, P. N.; Webster, M. *J. Chem. Soc., Dalton Trans*. **1996**, 823−828.
(5) Nakano, M.; Kuroda, A.; Maikawa, T.; Matsubayashi, G. *Mol. Cryst. Liq. Cryst.* **1996**, *284*, 301−305.
(6) Kumasaki, M.; Tanaka, H.; Kobayashi, A. *J. Mater. Chem.* **1998**, *8*, 301−307.
(7) Ueda, K.; Goto, M.; Iwamatsu, M.; Sugimoto, T.; Endo, S.; Toyota, N.; Yamamoto, K.; Fujita, H. *J. Mater. Chem.* **1998**, *8*, 2195−2198.
(8) Ueda, K.; Kamata, Y.; Iwamatsu, M.; Sugimoto, T.; Fujita, H. *J. Mater. Chem*. **1999**, *9*, 2979−2983.
(9) (a) Kobayashi, A.; Tanaka, H.; Kumasaki, M.; Torii, H.; Narymbetov, B.; Adachi, T. *J. Am. Chem. Soc*. **1999**, *121*, 10763−10771. (b) Kobayashi, A.; Kumasaki. M.; Tanaka, H. *Synth. Met.* **1999**, *102*, 1768−1769.
(10) Tanaka, H.; Okano, Y.; Kobayashi, H.; Suzuki, W.; Kobayashi, A. *Science* **2001**, *291*, 285−287.
(11) (a) Kobayashi, A.; Tanaka, H.; Kobayashi, H. *J. Mater. Chem.* **2001**, *11*, 2078−2088. (b) Kobayashi, A.; Suzuki, W.; Fujiwara, E.; Otsuka, T.; Tanaka, H.; Okano, Y.; Kobayashi, H. *Mol. Cryst. Liq. Cryst.* **2002**, *379*, 19−28.
(12) Kobayashi, A.; Fujiwara, E.; Kobayashi, H. *Chem. Rev*. **2004**, *104*, 5243−5264.
(13) Tanaka, H.; Tokumoto, M.; Ishibashi, S.; Graf, D.; Choi, E. S.; Brooks, J. S.; Yasuzuka, S.; Okano, Y.; Kobayashi, H.; Kobayashi, A. *J. Am. Chem. Soc*. **2004**, *126*, 10518−10519.
(14) Rovira, C.; Novoa, J. J.; Mozos, J.-L.; Ordejón, P.; Canadell, E. *Phys. Rev. B: Condens. Matter Mater. Phys.* **2002**, *65*, 081104-1−081104-4.
(15) Suzuki, W.; Fujiwara, E.; Kobayashi, A.; Fujishiro, Y.; Nishibori, E.; Takata, M.; Sakata, M.; Fujiwara, H.; Kobayashi, H. *J. Am. Chem. Soc.* **2003**, *125*, 1486−1487.
(16) Zhou, B.; Shimamura, M.; Fujiwara, E.; Kobayashi, A.; Tanaka, H.; Nishibori, E.; Sakata, M.; Cui, H.; Takahashi, K.; Kobayashi, H. *J. Am. Chem. Soc.* **2006**, *128*, 3872−3873.
(17) Tanaka, H.; Hara, S.; Tokumoto, M.; Kobayashi, A.; Kobayashi, H., *Chem. Lett.* **2007**, *36*, 1006−1007.
(18) Ishibashi, S.; Tanaka, H.; Kohyama, M.; Tokumoto, M.; Kobayashi, A.; Kobayashi, H.; Terakura, K. *J. Phys. Soc. Jpn.* **2005**, *74*, 843−846.
(19) Tanaka, H.; Kobayashi, H.; Kobayashi, A. *J. Am. Chem. Soc.* **2002**, *124*, 10002−10003.
(20) Kobayashi, A.; Kato, R.; Kobayashi, H.; Moriyama, S.; Nishio, Y.; Kajita, K.; Sasaki, W. *Chem. Lett.* **1987**, 459−462.
(21) Fujiwara, E.; Kobayashi, A.; Fujiwara, H.; Kobayashi, H. *Inorg. Chem.* **2004**, *43*, 1122−1129.
(22) Tanaka, H.; Kobayashi, H.; Kobayashi, A. *Synth. Met.* **2003**, *135−136*, 549−550.

Chart 1

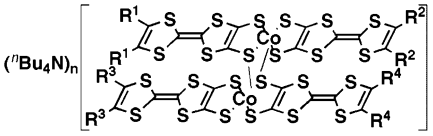

1; $2R^1$, $2R^2$, $2R^3$, $2R^4$ = -$(CH_2)_4$-, n = 2
2; R^1, R^2, R^3, R^4 = -Me, n = 2
3; R^1, R^2, R^3, R^4 = -Me, n = 0
4; R^1, R^2, R^3, R^4 = -H, n = 0

$(dt)_2]_2$ was performed by synchrotron powder diffraction experiments at SPring-8 using the revised GA (genetic algorithm)/MEM (maximum entropy method) method.[23] This is a rare case where the nontrivial molecular and crystal structures are successfully determined by X-ray powder diffraction experiments.

Experimental Section

General Methods. The corresponding TTF-dithiolate ligands—4,5-bis(2′-cyanoethylthio)-4,5-tetramethylene-TTF (**5**), 4,5-bis(2′-cyanoethylthio)-4,5-dimethyl-TTF (**6**), and 4,5-bis(2′-cyanoethylthio)-TTF (**7**)—were successfully prepared by a pseudo-Wittig reaction according to a procedure described in the literature.[24] Tetrahydrofuran (THF) was freshly distilled under argon atmosphere over sodium and benzophenone prior to use. Methanol (MeOH) was distilled under argon atmosphere over magnesium methoxide. Cobalt(II) chloride hexahydrate was recrystallized several times with distilled water and dried in air. The supporting electrolytes used in the electrocrystallization were recrystallized several times with ethyl acetate (AcOEt) and dried under reduced pressure. Chlorobenzene (PhCl) was washed three times with concentrated sulfuric acid and subsequently with aqueous sodium hydrogen carbonate solution and water, followed by drying over calcium chloride and distillation over diphosphorus pentaoxide under argon atmosphere. Acetonitrile (MeCN) was distilled under an argon atmosphere over calcium hydride. Benzonitrile (PhCN) was shaken several times with 2 N hydrochloric acid; subsequently, it was washed with water, aqueous sodium hydrogen carbonate solution, and water again, followed by drying with calcium chloride, and distilled over diphosphorus pentaoxide under an atmosphere of dry argon. All the other reagents were used without purification. The microanalyses were performed by the Research Center for Molecular-scale Nanoscience, Institute for Molecular Science.

Syntheses. Synthesis of $(Me_4N)_{2n}[Co(chdt)_2]_n$ ($n = 1$ or 2) (11). Ligand **5** (215 mg; 0.502 mmol) was hydrolyzed with a 25 wt % MeOH solution of tetramethylammonium hydroxide (730 mg; 2.00 mmol) in dry THF (15.0 mL) at room temperature and under an argon atmosphere. The color of the solution changed from orange to red as the reaction proceeded. The solution was stirred for 1 h, resulting in a reddish-orange precipitate **8**. A solution of cobalt(II) dichloride hexahydrate (64.2 mg; 0.270 mmol) in dry MeOH (4.0 mL) was added dropwise to the reaction mixture at −78 °C, and the reaction mixture was stirred for 1 h at the same temperature and warmed to room temperature overnight. The resulting microcrystals were collected by filtration and washed three times with a mixed solvent of dry THF (10.0 mL) and dry MeOH (1.0 mL) at 0 °C under an argon atmosphere to afford purple-gray microcrystals of **11**. Microanalysis and estimation of the yield could not be performed due to its highly air-unstable nature.

Synthesis of $(Me_4N)_{2n}[Co(dmdt)_2]_n$ ($n = 1$ or 2) (12). Complex **12** was synthesized through intermediate **9** using a method almost similar to that of the case of complex **11** from **6** (200 mg; 0.574 mmol), a 10 wt % MeOH solution of tetramethylammonium hydroxide (2.19 g; 2.40 mmol) in dry THF (12.0 mL) and a solution of cobalt(II) dichloride hexahydrate (69.0 mg; 0.290 mmol) in dry MeOH (5.0 mL) as air-unstable reddish-purple microcrystals. Microanalysis and estimation of the yield could not be performed because of its highly air-unstable nature.

Synthesis of $(Me_4N)_{2n}[Co(dt)_2]_n$ ($n = 1$ or 2) (13). Complex **13** were obtained through intermediate **10** by a procedure similar to that for the synthesis of complex **11** from **7** (188 mg; 0.502 mmol), a 25 wt % MeOH solution of tetramethylammonium hydroxide (732 mg; 2.01 mmol) in dry THF (15.0 mL) and a solution of cobalt(II) dichloride hexahydrate (61.2 mg; 0.257 mmol) in dry MeOH (4.0 mL) as air-unstable purple-gray microcrystals. Even in the case of **13**, microanalysis and estimation of the yield could not be performed because of its easy air-oxidation.

Electrochemical Synthesis. All the electrocrystallizations were performed in a standard H-type cell without a glass frit using two platinum electrodes of 1 mm ϕ under argon atmosphere. Four types of cobalt complexes (**1**−**4**) were obtained.

Preparation of $(^nBu_4N)_2[Co(chdt)_2]_2$ (1). Complex **11** (15.0−20.0 mg; 17.7−23.6 × 10^{-3} mmol calculated for $n = 1$) and tetra-*n*-butylammonium hexafluorophosphate (80.0 mg; 0.206 mmol) were dissolved in dry PhCl (12.0 mL) under an argon atmosphere. Electrochemical oxidation of this solution was performed with a constant current of 0.3 μA at room temperature. Comparatively air-stable block-shaped black single crystals of **1** grew on the anode within approximately 3 weeks. The obtained block-shaped black crystals were filtered, washed with ethanol (EtOH), and air-dried at room temperature. Anal. Calcd for $C_{72}H_{104}S_{24}Co_2N_2$: C, 45.88; H, 5.56; N, 1.49. Found: C, 45.63; H, 5.71; N, 1.62.

Preparation of $(^nBu_4N)_2[Co(dmdt)_2]_2$ (2) and Neutral $[Co(dmdt)_2]_2$ (3). Complex **12** (15.0−20.0 mg; 18.8−25.1 × 10^{-3} mmol calculated for $n = 1$) and tetra-*n*-butylammonium hexafluorophosphate (120.0 mg; 0.310 mmol) were dissolved in dry MeCN (18.0 mL) under an argon atmosphere. Electrochemical oxidation of this solution was carried out with a constant current at room temperature. After the application of a constant current of 0.3 μA for 8 weeks, comparatively air-stable block-shaped dark-red single crystals of **2** grew on the anode. The obtained crystals were filtered, washed with cold (0 °C) EtOH, and air-dried at room temperature. Anal. Calcd for $C_{64}H_{96}S_{24}Co_2N_2$: C, 43.16; H, 5.43; N, 1.57. Found: C, 45.63; H, 5.71; N, 1.62. On the other hand, **3** was prepared as air-stable plate-shaped black crystals by applying a constant current of 0.6 μA for 3 weeks. Anal. Calcd for $C_{32}H_{24}S_{24}Co_2$: C, 29.66; H, 1.87; N, 0.00. Found: C, 29.31; H, 1.76; N, 0.00.

Preparation of $[Co(dt)_2]_2$ (4). Neutral species **4** was prepared by using **13** (15.0−30.0 mg; 20.2−27.0 × 10^{-3} mmol calculated for $n = 1$) and tetra-*n*-butylammonium perchlorate (80.0 mg; 23.4 mmol) in dry PhCN (15.0 mL). After the application of a constant current of 0.5 μA at room temperature, air-stable needle-shaped black microcrystals of **4** grew on the anode within approximately 3 weeks. Anal. Calcd for $C_{24}H_8S_{24}Co_2$: C, 24.35; H, 0.68; N, 0.00. Found: C, 24.47; H, 0.86; N, 0.00.

Crystal Structure Determination. X-ray Structure Determination of 1−3. Single-crystal X-ray structure determination was performed on the crystals of **1**−**3**. The crystal data and experimental details of the crystal structure determination are listed in Table 1.

(23) Sakata, M.; Nishibori, E. Japanese Patent 2005350770 (2005).
(24) (a) Binet, L.; Fabre, J. M.; Montginoul, C; Simonsen, K. B.; Becher, J. *J. Chem. Soc., Perkin Trans. 1* **1996**, 783−788. (b) Binet, L.; Montginoul, C.; Fabre, J. M.; Ouahab, L.; Golhen, S.; Becher, J. *Synth. Met.* **1997**, *86*, 1825−1826.

Table 1. X-ray Crystallographic Data of the Cobalt Complexes **1**−**3**

	(^{n}Bu$_4$N)$_2$[Co(chdt)$_2$]$_2$ (**1**)	(^{n}Bu$_4$N)$_2$[Co(dmdt)$_2$]$_2$ (**2**)	[Co(dmdt)$_2$]$_2$ (**3**)
formula	$C_{36}H_{52}S_{12}CoN$	$C_{32}H_{48}S_{12}CoN$	$C_{16}H_{12}S_{12}Co$
fw	942.47	890.39	647.91
cryst color, habit	black, block	black, block	black, plate
cryst syst	triclinic	triclinic	monoclinic
lattice parameters			
a (Å)	11.235(2)	11.955(4)	7.4608(5)
b (Å)	12.214(3)	13.452(5)	28.245(2)
c (Å)	17.701(5)	15.042(3)	10.7208(7)
α (°)	83.05(2)	111.14(2)	
β (°)	81.39(2)	103.37(2)	93.360(1)
γ (°)	65.82(2)	102.36(3)	
V (Å^3)	2186.0(9)	2073(1)	2255.3(3)
space group	$P\bar{1}$ (No. 2)	$P\bar{1}$ (No. 2)	$P2_1/n$ (No. 14)
Z value	2	2	4
D_{calc} (g·cm^{-3})	1.432	1.426	1.908
μ(Mo Kα) (cm^{-1})	9.94	10.43	18.77
diffractometer	Rigaku/MSC Mercury CCD	Bruker Smart APEX CCD	Bruker Smart APEX CCD
radiation	Mo Kα (λ = 0.71070 Å)	Mo Kα (λ = 0.71073 Å)	Mo Kα (λ = 0.71073 Å)
T (K)	296	293	293
no. of reflns measd			
total	43 690	8651	14 090
unique	9654		
structure solution	direct methods (*SIR2002*)	direct methods (*SHELXS97*)	direct methods (*SHELXS97*)
refinement	full-matrix least squares	full-matrix least squares	full-matrix least squares
no. observations	4493 [$I > 5.00\sigma(I)$]	4771 [$I > 3.00\sigma(I)$]	5222 [$I > 2.00\sigma(I)$]
no. variables	503	415	266
residuals: R_1;[a] R_2[b]	0.067; 0.089	0.044; 0.051	0.041; 0.105
GOF indicator	1.627	1.130	1.051

[a] $R_1 = \sum||F_o| - |F_c||/\sum|F_o|$. [b] $R_2 = [\sum\omega(|F_o| - |F_c|)^2/\sum\omega F_o^2]^{1/2}$.

The data collection for **1** was performed on a Rigaku/MSC APEX Mercury CCD system and that for **2** and **3** was performed on a Bruker Smart CCD system with graphite-monochromated Mo Kα radiation (λ = 0.71070 Å for **1** and λ = 0.71073 Å for **2** and **3**) at 293 K. The crystal structures were determined by direct methods.[25−28] The atomic scattering factors were obtained from the International Tables for X-ray Crystallography.[29] Anisotropic temperature factors were applied to the non-hydrogen atoms. The calculated positions of the hydrogen atoms were not refined but were included in the final calculation. All the calculations were performed using the *CrystalStructure* crystallographic software package[30] and *SHELX97*.[27,31]

X-ray Powder Diffraction for 4. The synchrotron radiation X-ray powder diffraction experiment was performed on the neutral complex **4** to obtain the information on the crystal structure. Crystal data: $C_{12}H_4S_{12}Co_1$, M = 589.976, triclinic, space group $P\bar{1}$, a = 11.7164(2) Å, b = 10.9496(1) Å, c = 7.7319(7) Å, α = 79.731(1)°, β = 96.481(2)°, γ = 113.9686(9)°, V = 890.96(3) Å^3, and Z = 2. The experiment was carried out by using imaging plate detectors and a large Debye−Scherrer camera at the facility of SPring-8 BL02B2. The wavelength of the incident X-rays was 1.00088 Å. The exposure time was 120 min. An ideal X-ray powder pattern was obtained for every step of 0.01° for 2θ values ranging from 4.0° to 72.0°. The structure was solved by a modified genetic algorithm (GA)[23] and refined by the MEM/Rietveld method.[32,33] The final R factors after the Rietveld analysis are R_{wp} = 0.036 and R_I = 0.064.

Static Magnetic Susceptibility Measurements. Static magnetic susceptibility (χ) measurements of complexes **1** (0.60 mg; 3.18 × 10^{-4} mmol), **2** (9.01 mg; 5.06 × 10^{-3} mmol), **3** (5.00 mg; 3.86 × 10^{-3} mmol), and **4** (2.95 mg; 2.49 × 10^{-3} mmol) were performed with a Quantum Design MPMS-7XL superconducting quantum interference device (SQUID) magnetometer in the temperature range from 1.9 to 300 K. The applied magnetic fields were 30 kOe for the tetra-*n*-butylammonium salt **1** and 5 kOe for compounds **2**−**4**. The samples were wrapped in a clean aluminum foil whose magnetic susceptibility was separately measured and subtracted. The diamagnetic contribution was calculated from Pascal's constants (χ^{dia} = −1.13 × 10^{-3}, −1.05 × 10^{-3}, −8.72 × 10^{-4}, and −8.53 × 10^{-4} emu·mol^{-1} for **1**, **2**, **3**, and **4**, respectively).

Electrical Resistivity Measurements of 3 and 4. The electrical resistivities were measured on tiny single crystals (250 × 150 × 20 μm) of **3** and on a compressed pellet sample of **4** by a four-probe technique. The measurements were performed with a

(25) *SIR2002*: Burla, M. C.; Camalli, M.; Carrozzini, B.; Cascarano, G. L.; Giacovazzo, C.; Polidori, G.; Spagna, R. *J. Appl. Crystallogr*. **2003**, *36*, 1103−1103.

(26) *DIRDIF99*: Beurskens, P. T.; Admiraal, G.; Beurskens, G.; Bosman, W. P.; de Gelder, R.; Israel, R; Smits, J. M. M. The *DIRDIF-99 Program System*; Technical Report of the Crystallography Laboratory, University of Nijmegen: Nijmegen, The Netherlands, 1999.

(27) *SHELXS-97*: Sheldrick, G. M. *SHELXS-97*. *Program for Crystal Structure Solution*; University of Göttingen: Göttingen, Germany, 1990.

(28) *DIRDIF94*: Beurskens, P. T.; Admiraal, G.; Beurskens, G.; Bosman, W. P.; de Gelder, R.; Israel, R.; Smits, J. M. M. *The DIRDIF-94 Program System*; Technical Report of the Crystallography Laboratory, University of Nijmegen: Nijmegen, The Netherlands, 1994.

(29) Cromer, D. T.; Waber, J. T. In *International Tables for X-ray Crystallography*; The Kynoch Press: Birmingham, England, 1974; Table 2.2 A, Vol. IV.

(30) (a) *CrystalStructure 3.5.1: Crystal Structure Analysis Package*; Rigaku and Rigaku/MSC: The Woodlands TX, 2000−2003. (b) *CRYSTALS Issue 10*: Watkin, D. J.; Prout, C. K.; Carruthers, J. R.; Betteridge, P. W. Chemical Crystallography Laboratory: Oxford, U.K., 1996.

(31) (a) *SHELX97:* Sheldrick, G. M. *SHELX 97, Programs for Crystal Structure Analysis*: University of Göttingen: Göttingen, Germany, 1998. (b) *SHELXL-97*: Sheldrick, G. M. *SHELXL-97 Program for the Refinement of Crystal Structures from Diffraction Data*; University of Göttingen: Göttingen, Germany, 1997.

(32) Kariuki, B. M.; Serrano-González, H.; Johnston, R. L.; Harris, K. D. M. *Chem. Phys. Lett*. **1997**, *280*, 189−195.

(33) (a) Takata, M.; Umeda, B.; Nishibori, E.; Sakata, M.; Saito, Y.; Ohno, M.; Shinohara, H. *Nature* **1995**, *377*, 46−49. (b) Takata, M.; Nishibori, E.; Sakata, M. *Z. Kristallogr*. **2001**, *216*, 71−86.

Table 2. Exponents (ζ) and Ionization Potentials (E_i) for Atomic Orbitals

	orbital	ζ	E_i (eV)		orbital	ζ	E_i (eV)
S	3s	2.122	−22.0	C	2s	1.625	−21.4
	3p	1.827	−10.5		2p	1.625	−11.4
Co	4s	2.0	−9.21	H	1s	1.0	−13.6
	4p	2.0	−5.29				
	3d	[a]	−13.2				

[a] Double ζ: $0.5679\chi_1(5.55) + 0.6059\chi_2(2.1)$.

Scheme 1[a]

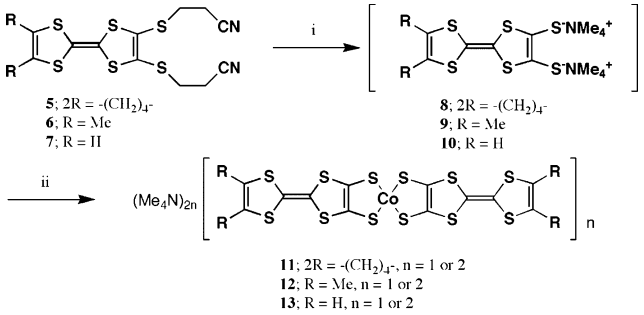

[a] Reagents and conditions: (i) 10 wt or 25 wt % Me_4NOH/MeOH (4.0−4.2 equiv), dry THF, rt, 1 h; (ii) $Co(II)Cl_2 \cdot 6H_2O$/dry MeOH (0.5 equiv), −78 °C to rt, overnight.

Quantum Design PPMS down to 1.9 K for **3** and a Huso Electro Chemical System HECS 994C-1 multichannel four-terminal conductometer down to 0.55 K for **4**. Electrical contacts were achieved using gold paste and gold wires (15 μm ϕ). In the latter case, the samples were cooled to 1.5 K by pumping liquid ^{4}He, and the experiments below 1.5 K were performed by pumping liquid ^{3}He. A calibrated Cernox thermometer was used for the entire temperature range.

Band Structure Calculation of 4. The electronic band structures of **4** were calculated using the extended Hückel tight-binding approximation on the basis of the HOMO and LUMO. The exponents (ζ) and the ionization potentials (E_i) for the atomic orbitals are listed in Table 2.

Results and Discussion

Syntheses. The syntheses of cobalt complexes **11**−**13** (n = 1 or 2) were performed under a strictly inert atmosphere using a Schlenk technique by a procedure shown in Scheme 1. In the TTF derivatives **5**−**7**, cyanoethyl groups are used to protect a dithiolate ligand function and can be removed with an excess of basic reagents. The deprotection of the cyanoethyl group generates the coordination ability of the dithiolate ligands toward a central metal atom.[3−8,34] The tetramethylammonium dithiolate ligands $(Me_4N^+)_2(chdt^{2-})$ (**8**), $(Me_4N^+)_2(dmdt^{2-})$ (**9**), and $(Me_4N^+)_2(dt^{2-})$ (**10**) were generated as reddish-orange or pink precipitates by the deprotection of **5**, **6**, and **7**, respectively, with a MeOH solution of tetramethylammonium hydroxide in dry THF at room temperature. Complexes **11**−**13** were obtained by the successive treatment of **8**−**10**, respectively, with a dry MeOH solution of cobalt(II) dichloride hexahydrate from −78 °C to room temperature. The resulting purple-gray or reddish-purple precipitates of **11**−**13** were collected and washed several times with a dry THF−MeOH (v/v = 10:1) solution. The obtained complexes **11**−**13** were easily air-oxidized and dissolved in common organic solvents.

We have attempted many preparations of crystals under various conditions of electrocrystallization by varying the supporting electrolytes, solvents, concentrations of the reagents, temperatures, and currents and voltages to afford good single crystals. Crystals of **1** can be prepared by an electrochemical oxidation of **11** in the presence of tetra-*n*-butylammonium hexafluorophosphate in dry PhCl at room temperature. Black block-shaped single crystals grew on the anode within approximately 3 weeks by applying a constant current of 0.3 μA. On the other hand, **4** was also electrochemically obtained from **13** as very small black needle-shaped crystals from a dry PhCN solution containing tetra-*n*-butylammonium perchlorate by applying a constant current of 0.5 μA at room temperature. Crystals of **2** and **3** were also obtained by the electrochemical oxidation of **12** in MeCN containing tetra-*n*-butylammonium hexafluorophosphate as the electrolyte under constant currents of 0.3 and 0.6 μA, respectively. Dark-red block-shaped crystals of **2** and black plate-shaped crystals of **3** grew on the anode.

Crystal Structure Determination. Although the reflection data of **1**−**3** were successfully obtained by using the usual CCD diffractometers, the single-crystal X-ray structure analysis of **4** could not be carried out due to the small size of the obtained crystals. Therefore, a synchrotron radiation X-ray powder diffraction experiment was performed on **4** using the imaging plate detectors and a large Debye−Scherrer camera at the facility of SPring-8 BL02B2. The structure of $[Co(dt)_2]_2$ was determined by use of the modified GA and MEM/Rietveld method.[23,32,33] This is a rare example of the structure determination of metal complexes whose crystal structure is determined by X-ray powder diffraction without any initial information on the structure.[35]

Crystal Structure of 1. As shown in Figure 1a, the crystal structure analysis of the tetra-*n*-butylammonium salt of **1** revealed that one tetra-*n*-butylammonium cation and one-half of the $[Co(chdt)_2]_2^{2-}$ anion are crystallographically independent. The molecular structure of the $[Co(chdt)_2]_2^{2-}$ anion of **1** is shown in Figure 1b. Two $[Co(chdt)_2]$ units that are related to each other by a center of inversion (symmetry operation $2 - x$, $1 - y$, $1 - z$) are strongly dimerized with an interplanar distance of 3.26 Å and slip distances of 1.53 and 1.43 Å along the molecular long and short axes, respectively. They are connected to each other by two apical Co1−S2* and Co1*−S2 bonds (2.348 Å) similar to those of the other cobalt dithiolene complexes.[22,36] The average basal Co−S bond length in the $[Co(chdt)_2]$ unit is 2.215 Å, and the Co1···Co1* distance is 3.200 Å between the adjacent units. The Co−S−Co angle (89.1°) is almost 90°. Conse-

(34) Misaki, Y.; Tani, Y.; Taniguchi, M.; Maitani, T.; Tanaka, K.; Bechgaard, K. *Mol. Cryst. Liq. Cryst.* **2000**, *343*, 377−382.

(35) For example: Suzuki, W.; Fujiwara, E.; Kobayashi, A.; Fujishiro, Y.; Nishibori, E.; Takata, M.; Sakata, M.; Okano, Y.; Kobayashi, H. *Chem. Lett.* **2003**, *32*, 1106−1107.

(36) For example: (a) Welch, J. H.; Bereman, R. D.; Singh, P.; Moreland, C. *Inorg. Chim. Acta* **1989**, *158*, 17−25. (b) Balch, A. L.; Dance, I. G.; Holm, R. H. *J. Am. Chem. Soc.* **1968**, *90*, 1139−1145. (c) Schrauzer, G. N.; Mayweg, V. P.; Finck, H. W.; Heinrich, W. *J. Am. Chem. Soc.* **1966**, *88*, 4604−4609.

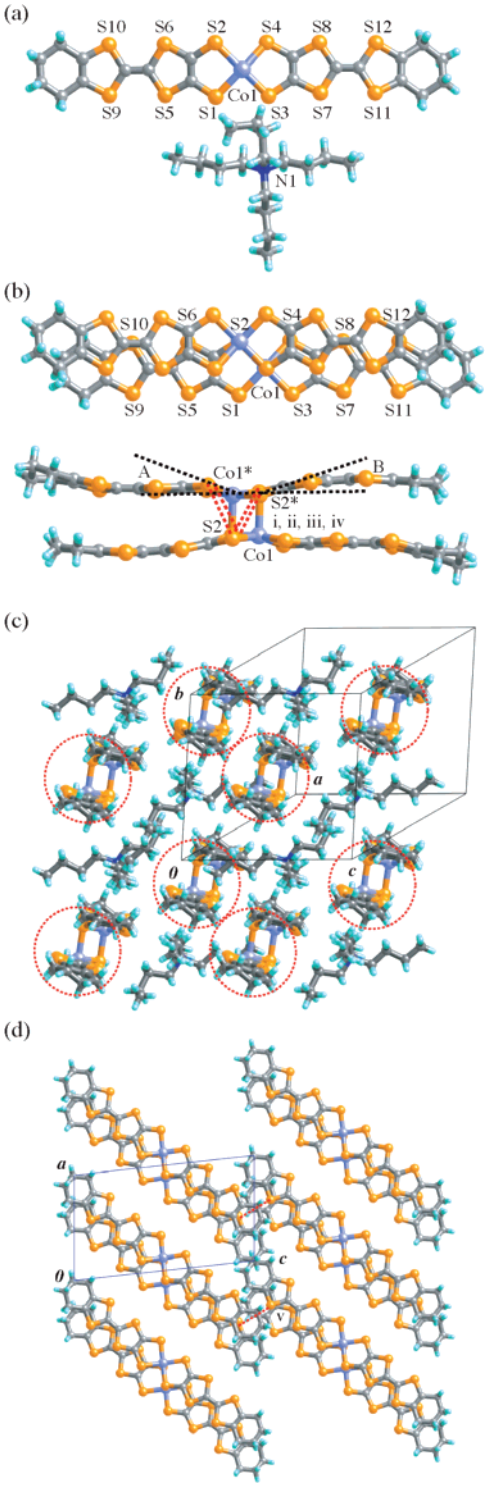

Figure 1. (a) Crystallographically independent molecules in **1**. (b) Molecular structures of the anion molecule in **1**. Intramolecular contacts are (i) S2···S1* = 3.381 Å, (ii) S2···S2* = 3.250 Å, (iii) S2···S3* = 3.377 Å, and (iv) S2···S4* = 3.591 Å. Dihedral angles are $A = 26.68°$ and $B = 16.80°$. The interplanar distance is 3.26 Å, and slip distances are 1.53 and 1.43 Å along the molecular long and short axes, respectively, between the $[Co(chdt)_2]$ units within the dimerized $[Co(chdt)_2]_2^{2-}$ anion. (c) Crystal structure of **1** viewed along the long axis of the anion molecule. The anion molecules are surrounded by the dotted circles in Figure 1c. (d) Anion arrangement projected onto the *ac* plane in **1**. The bulky tetra-*n*-butylammonium cations are omitted for clarity in Figure 1d. The intermolecular contact is (v) S12···S12* = 3.567 Å.

quently, $(^nBu_4N)[Co(chdt)_2]$ should be appropriately described as a dimerized complex, $(^nBu_4N)_2[Co(chdt)_2]_2$ (see Figure 1a,b). As shown in Figure 1b, the central cobalt atom has a slightly distorted square-pyramidal coordination geometry. Within each $[Co(chdt)_2]$ unit, the cobalt atom is displaced from the optimal plane of the four sulfur atoms around the cobalt atom by approximately 0.25 Å toward the apical sulfur atom of the other $[Co(chdt)_2]$ unit of the dimer. As Figure 1b also indicates, the two ligand parts connected to the central metal are crooked and adopt a butterfly-wing-shaped conformation, probably to relieve the steric hindrance of the terminal cyclohexeno ring. There are many short S···S contacts whose lengths are less than the sum of the van der Waals radii of the sulfur atom (3.7 Å) in the $[Co(chdt)_2]_2^{2-}$ anion within the dimeric structure, as described in the caption of Figure 1b. The crystal structure of $(^nBu_4N)_2[Co(chdt)_2]_2$ is shown in Figure 1c. Neither a stacking nor a columnar structural arrangement of the $[Co(chdt)_2]_2^{2-}$ anion is observed. The nearest six positions around the $[Co(chdt)_2]_2^{2-}$ anion are occupied by the bulky tetra-*n*-butylammonium cations. Figure 1d shows the arrangement of the $[Co(chdt)_2]_2^{2-}$ anions viewed along the *b* axis. Despite this isolated structure surrounded by the bulky tetra-*n*-butylammonium cations, only one S···S contact (S12···S12* = 3.567 Å) between the adjacent $[Co(chdt)_2]_2^{2-}$ anions is found along the [011] direction, as indicated by a dotted line in Figure 1d. On the other hand, the shortest intermolecular Co···Co distance of 8.209 Å is observed between the $[Co(chdt)_2]_2^{2-}$ anions arranged along the *a* axis. With respect to the anion chain along the [011] direction, the shortest intermolecular Co···Co distance is 18.174 Å.

Crystal Structure of 2. As shown in Figure 2a, one tetra-*n*-butylammonium cation and one-half of the $[Co(dmdt)_2]_2^{2-}$ anion are crystallographically independent. Two $[Co(dmdt)_2]$ units are related by a center of inversion (symmetry operation $1 - x, 1 - y, 1 - z$), and a central cobalt atom is coordinated by a sulfur atom of the adjacent $[Co(dmdt)_2]$ unit. Therefore, the central cobalt atom has a distorted square-pyramidal coordination geometry. The apical Co1−S8* bond length (2.327 Å) is slightly shorter than those of complexes **1**, **3**, and **4** because the two dmdt ligands of the $[Co(dmdt)_2]$ unit are twisted by 19.7° to each other and the S8* atom comes close to the Co1 atom, as shown in Figure 2b. The average basal Co−S bond length in the $[Co(dmdt)_2]$ unit is 2.215 Å, and the Co1···Co1* distance is 3.335 Å between the adjacent units. The Co−S−Co angle (94.3°) is marginally larger than 90°. The molecular arrangement of **2** is shown in Figure 2c,d. The dimeric $[Co(dmdt)_2]_2^{2-}$ anions are arranged making their molecular long axes parallel to each other and form one-dimensional chains in a diagonal side-by-side direction. Tetra-*n*-butylammonium cations occupy the rest of the space. There are very short S···S contacts in the $[Co(dmdt)_2]_2^{2-}$ anion within the dimeric structure, as exhibited in Figure 2b. However, there is no short S···S contact between the $[Co(dmdt)_2]_2^{2-}$ anions; hence, each $[Co(dmdt)_2]_2^{2-}$ anion is isolated. The shortest intermolecular Co···Co distance of 11.715 Å is observed between the $[Co(dmdt)_2]_2^{2-}$ anions arranged along the *a* axis, as shown in Figure 2d.

Crystal Structure of Neutral 3. The molecular structure of the dimeric complex **3** is shown in Figure 3a. One-half

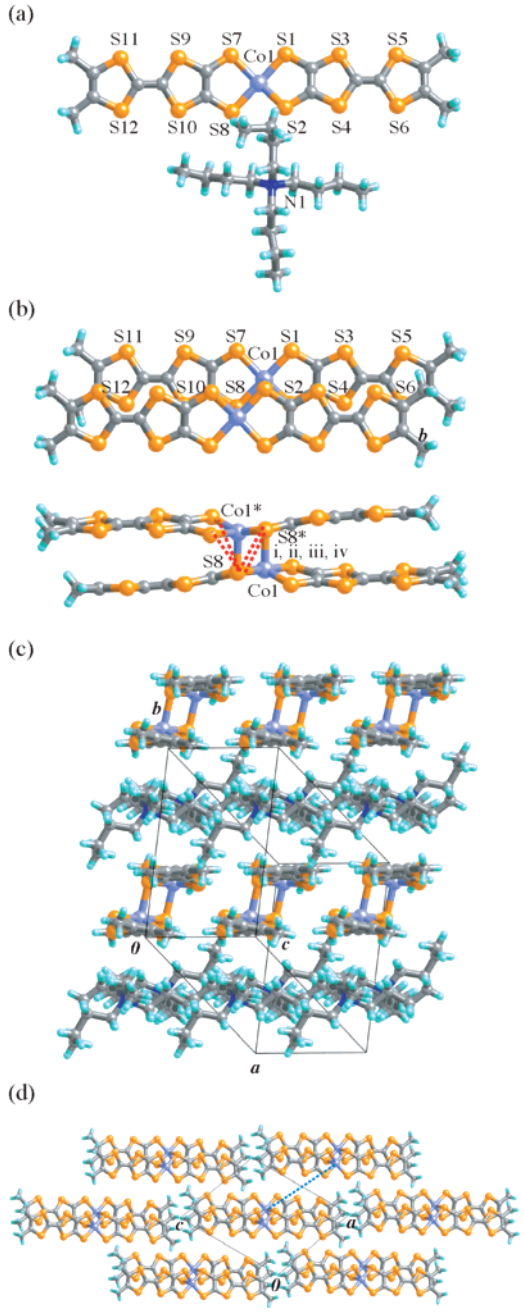

Figure 2. (a) Crystallographically independent molecules in **2**. (b) Molecular structures of the anion molecule in **2**. Intramolecular contacts are indicated as dotted lines: (i) S8···S8* = 3.086 Å, (ii) S8···S1* = 3.375 Å, (iii) S8···S2* = 3.534 Å, and (iv) S8···S7* = 3.565 Å. The dihedral angle between the twisted ligands is 19.7°. The interplanar distance is 3.39 Å, and slip distances are 1.57 and 1.72 Å along the molecular long and short axes, respectively, between the $[Co(dmdt)_2]$ units within the dimerized $[Co(dmdt)_2]_2^{2-}$ anion. (c) Crystal structure of **2** viewed along the molecular long axis of the anion molecule. (d) Anion arrangement projected onto the molecular plane. The bulky tetra-*n*-butylammonium cations are omitted for clarity. The interdimer Co···Co distance (11.715 Å) is indicated by a dotted line.

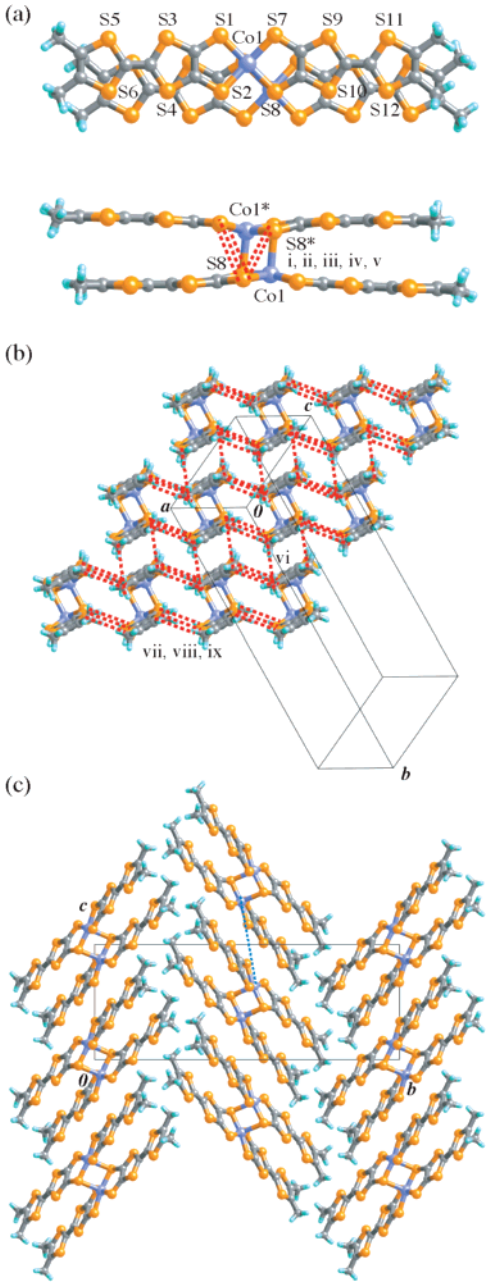

Figure 3. (a) Dimerized structures and atomic numbering schemes of **3**. Intramolecular contacts are indicated by dotted lines: (i) S8···S8* = 3.392 Å, (ii) S8···S1* = 3.404 Å, (iii) S8···S7* = 3.509 Å, (iv) S8···S2* = 3.518 Å, and (v) S7···S2* = 3.677 Å. The intramolecular interplanar distance between the $[Co(dmdt)_2]$ units within the dimerized $[Co(dmdt)_2]_2$ molecule is 3.23 Å, and slip distances are 1.43 and 1.53 Å along the molecular long and short axes, respectively. (b) Arrangement of **3** viewed along the molecular long axis. Intermolecular contacts are: (vi) S3···S4* = 3.653 Å, (vii) S2···S7* = 3.652 Å, (viii) S4···S7* = 3.614 Å, and (ix) S1···S4* = 3.660 Å. The intermolecular interplanar distance is 3.41 Å, and slip distances are 9.06 and 1.13 Å for the molecular long and short axes, respectively, between the adjacent molecules in the stacking direction. (c) Crystal structure projected onto the *bc* plane. The interdimer Co···Co distance (8.021 Å) is indicated by a dotted line.

of the $[Co(dmdt)_2]_2$ molecule is crystallographically independent. The $[Co(dmdt)_2]_2$ molecule is required to be centrosymmetric with a center of inversion $(1 - x, -y, 2 - z)$ located exactly in the middle of the two cobalt atoms. As compared with that of **2**, the $[Co(dmdt)_2]$ unit has a higher planarity. Two TTF parts of the $[Co(dmdt)_2]$ unit are almost parallel to each other, but the central cobalt atom deviates by 0.28 Å from the least-squares plane that comprises the 12 sulfur atoms of the $[Co(dmdt)_2]$ unit. The apical Co1−S8* bond length is 2.405 Å, and the average basal Co−S bond length in the $[Co(dmdt)_2]$ unit is 2.199 Å. The Co1···Co1* distance in **3** is 3.124 Å. There are many short S···S contacts that are less than 3.7 Å in the [Co-

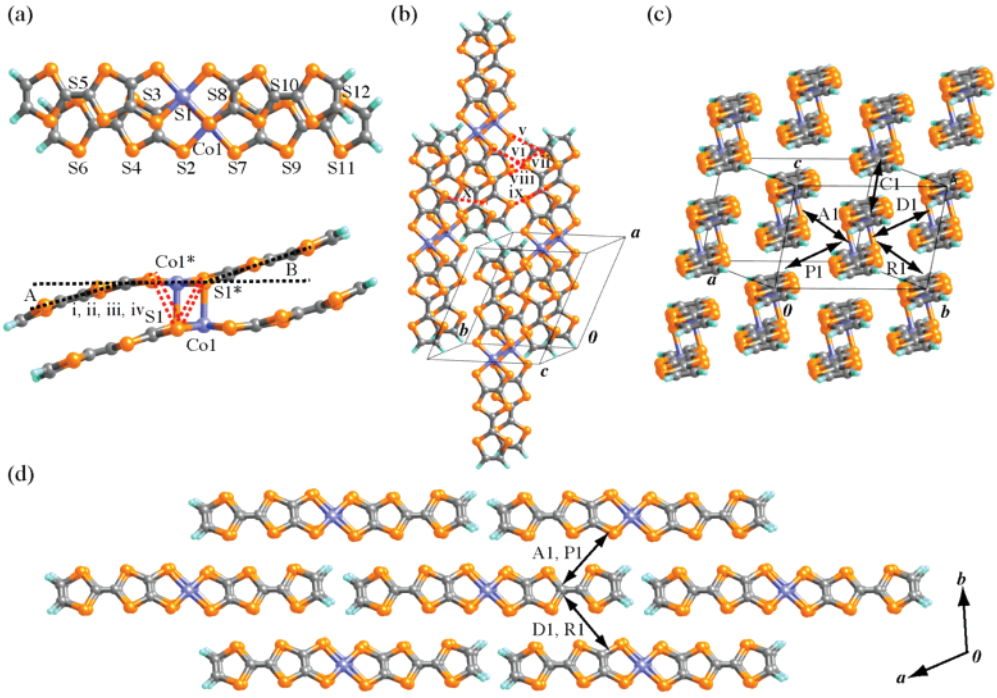

Figure 4. (a) Dimerized structures and atomic numbering schemes of **4**. Intramolecular contacts are: (i) S1···S1* = 3.239 Å, (ii) S1···S2* = 3.507 Å, (iii) S1···S7* = 3.413 Å, and (iv) S1···S8* = 3.333 Å. Dihedral angles are $A = 20.74°$ and $B = 25.13°$. The intramolecular interplanar distance between the $[Co(dt)_2]$ units within the dimerized $[Co(dt)_2]_2$ molecule is 3.14 Å, and slip distances are 1.28 and 1.66 Å along the molecular long and short axes, respectively. (b) Crystal structure of **4**. Intermolecular contacts are: (v) S2···S12* = 3.522 Å, (vi) S6···S8* = 3.407 Å, (vii) S4···S12* = 3.502 Å, (viii) S4···S6* = 3.566 Å, (ix) S6···S10* = 3.493 Å, and (x) S5···S3* = 3.354 Å. (c) Stacking structure of **4** viewed along the molecular long axis. The intermolecular interplanar distance between the adjacent molecules in the stacking direction is 3.43 Å, and slip distances are 0.95 and 1.74 Å for the molecular long and short axes, respectively. (d) Crystal structure projected onto the *ab* plane. Intermolecular overlap integrals (A1, C1, D1, P1, and R1 in Figure 2c,d) are listed in Table 4.

$(dmdt)_2]_2$ dimeric structure, as seen in Figure 3a. The molecular stacking structure of **3** viewed along the molecular long axis is shown in Figure 3b. The dimerized $[Co(dmdt)_2]_2$ molecules form two-dimensional (2D) layers where many short S···S contacts within 3.7 Å exist. The symmetry operation of a two-fold screw axis along the *b* axis forms a zigzag molecular arrangement, as shown in Figure 3c. The dihedral angle between the molecular planes in the neighboring molecular layers is 67.2°. Each 2D layer is isolated because there is no short S···S contact between the neighboring layers. As a result, 2D networks mediated by the sulfur atoms of the ligands are developed in the *ac* plane. The shortest intermolecular Co···Co distance of 7.461 Å is observed between the $[Co(dmdt)_2]_2$ molecules arranged along the *a* axis.

Crystal Structure of Neutral 4. The structures and numbering scheme of the dimeric complex **4** are shown in Figure 4a. The unit cell of **4** contains one crystallographically independent half of the $[Co(dt)_2]_2$ molecule. The $[Co(dt)_2]_2$ molecule is required to be centrosymmetric with a center of inversion operation $(2 - x, 1 - y, 1 - z)$ at the origin located halfway between the two cobalt atoms. Thus, the neutral $[Co(dt)_2]_2$ molecule also has the same dimerized structure as those of the complexes **1**−**3.** The dimerization occurs through the formation of two Co1−S1* bonds of 2.374 Å (the average basal Co−S bond length in the $[Co(dt)_2]$ unit is 2.174 Å.). The Co1···Co1* distance in the $[Co(dt)_2]_2$ molecule is 3.208 Å, the intradimer interplanar distance is 3.14 Å, and the slip distances are 1.28 and 1.66 Å along the molecular long and short axes, respectively. The TTF units of the ligands are essentially planar and almost parallel to each other, while each $[Co(dt)_2]$ unit bends at the sulfur atoms around the central cobalt atom to yield a rare chair conformation (see Figure 4a). The coordination geometry around the cobalt atom is square pyramidal wherein the cobalt shifts by 0.214 Å from the plane of the four basal sulfur atoms toward the apical sulfur. As shown in Figure 4a, several intramolecular S···S contacts exist through the sulfur atoms that are coordinated to the central cobalt atom. The cell-packing diagrams for the $[Co(dt)_2]_2$ molecule are shown in Figure 4b−d. The $[Co(dt)_2]_2$ molecules are arranged in a zigzag manner with respect to each other along the molecular long axis and the direction perpendicular to the molecular plane. Along the [001] direction, as shown in Figure 4c, each $[Co(dt)_2]_2$ molecule stacks with an interplanar distance of 3.43 Å and slip distances of 0.95 and 1.74 Å for the molecular long and short axes, respectively. No intermolecular S···S distance that is shorter than the sum of the van der Waals radii is observed along the stacking direction (the shortest intermolecular S···S distance in the molecular stacking direction is S4···S9* = 3.711 Å). As shown in Figure 4d, each molecule is surrounded by six neighboring $[Co(dt)_2]_2$ molecules that are located along the [100], [110], and [210] directions. There are many intermolecular S···S contacts between the molecules that are shorter than 3.7 Å along the [100] and [110] directions (see also Figure 4b,d). As a result, 2D networks mediated by the sulfur atoms of the ligands are developed in the *ab* plane, suggesting the

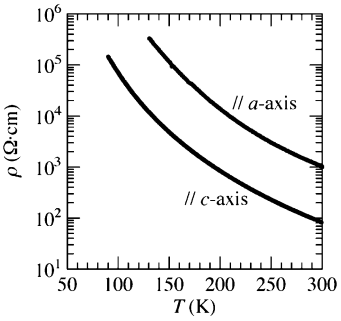

Figure 5. Temperature dependence of electrical resistivities measured on single crystals of **3** along the *a* and *c* axes. The room-temperature conductivities are 1.0×10^{-3} and 1.2×10^{-2} S·cm^{-1}, and the activation energies are estimated to be 118 and 85 meV along the *a* and *c* axes, respectively.

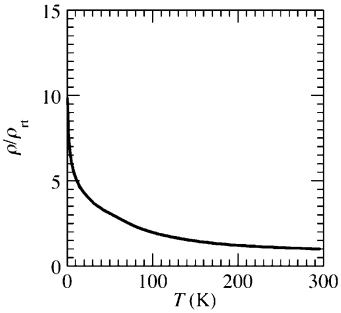

Figure 6. Temperature dependence of normalized electrical resistivities (ρ/ρ_{rt}) down to 0.55 K measured on a compressed pellet sample of **4**.

possibility of a high conductivity and stable metallic state in this complex. On the other hand, the shortest intermolecular Co···Co distance is 4.584 Å along the [001] direction (the molecular stacking direction).

Electrical Properties of Neutral 3 and Neutral 4. Neutral metal complexes with TTF-type dithiolate ligands usually have very small crystal sizes. However, the resistivity measurements could be performed on single crystals of **3** along the *a* and *c* axes because crystals with sufficiently large sizes for the usual four-probe measurements were obtained. However, **3** exhibited a semiconducting behavior (Figure 5). The room-temperature conductivities were 1.0×10^{-3} and 1.2×10^{-2} S·cm^{-1}, and the activation energies were estimated to be 118 and 85 meV along the *a* and *c* axes, respectively. On the other hand, the crystals of **4** were very small. Therefore, the electrical resistivity measurements were performed on a compressed pellet sample by the usual four-probe method down to 0.55 K, as shown in Figure 6. Neutral complex **4** showed a high room-temperature conductivity of 19 S·cm^{-1} despite the measurement on the compressed pellet sample, similar to the cases of the already-reported neutral metal complexes with TTF-type ditholate ligands.[22] It appears that such a high conductivity is realized by the 2D S···S network in the *ab* plane and the stacking structure of the $[Co(dt)_2]_2$ molecules (Figure 4). As seen from Figure 6, the resistivity increases extremely slowly with decreasing temperature (down to 0.55 K from room temperature) and retains a high conductivity even at 0.55 K ($\sigma_{0.55K}/\sigma_{rt}$ = ca. 1:10) despite the measurements performed on the compressed pellet sample. Consequently, it is highly possible that the single crystal of **4** is essentially metallic down to very low temperatures.

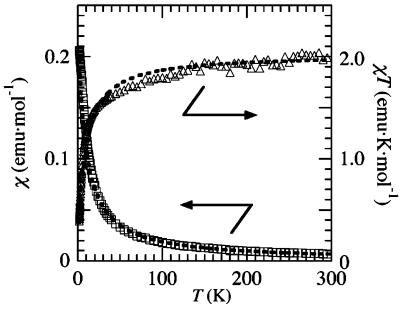

Figure 7. Temperature dependence of magnetic susceptibilities (χ) of randomly oriented polycrystals of **1** under 30 kOe. The dotted lines indicate fitting curves of the Curie−Weiss law ($C = 2.02$ K·emu·mol^{-1} and $\theta = -8.3$ K).

Magnetic Properties. The static magnetic susceptibility of **1** was measured by a SQUID magnetometer at 30 kOe. The room-temperature susceptibility after the correction of a diamagnetic contribution was 6.53×10^{-3} emu·mol^{-1} for the $(^nBu_4N)_2[Co(chdt)_2]_2$ formula unit. Figure 7 shows the temperature dependence of susceptibilities of **1** in the temperature range of 1.9−300 K. The susceptibilities of **1** can be well-fitted by Curie−Weiss law over the entire measured temperature range. The Curie constant ($C = 2.02$ K·emu·mol^{-1}) was equal to that of two $S = 1$ spins per formula unit ($C_{calc} = 2.02$ K·emu·mol^{-1} using the value of $g = 2.0116$ estimated by the electron spin resonance measurement of **1**), and the Weiss temperature indicates a slight antiferromagnetic interaction ($\theta = -8.3$ K). These results suggest that the intradimer magnetic interaction between $[Co(chdt)_2]^-$ monomers is considerably weaker and magnetic moments ($S = 1$ spins) exist without the compensation of spins in the dimer. One possible spin structure of **1** will be obtained as follows: (i) The cobalt(II) atom has a $S = {}^3/_2$ high-spin d^7 state, and the ligand site has no spin before the electrochemical oxidation of complex **11**. (ii) One $S = {}^1/_2$ spin is generated on the two ligand moieties of each $[Co(chdt)_2]$ unit by electrocrystallization. And (iii) the monomeric $[Co(chdt)_2]$ unit has a spin triplet ($S = 1$) state due to spin-pairing between one of the three cobalt spins and one π spin on the ligands. The resultant spin triplet state in the monomer was already suggested by R. Eisenberg et al.,[37] and DFT calculations by K. Ray et al. indicated that two unpaired spin orbitals of the $(^nBu_4N)[Co(^tBu_2bdt)_2]$ complex ($^tBu_2bdt$ = 3,5-di-*tert*-butylbenzene-1,2-dithiolate), $2b_{2g}$ and $2b_{3g}$, are constructed by the mixing of Co $3d_{xz}$-ligand b_{2g} and Co $3d_{yz}$-ligand b_{3g} orbitals, respectively.[38]

In the case of $[Co(dmdt)_2]_2$ complexes, the magnetic susceptibilities of the polycrystalline samples of **2** and **3** were measured at 5 kOe in the temperature range of 1.9−300 K using a SQUID magnetometer. The room-temperature susceptibility of **2** after the correction of a diamagnetic contribu-

(37) Eisenberg, R.; Dori, Z.; Gray, H. B.; Ibers, J. A. *Inorg. Chem.* **1968**, *7*, 741−748.
(38) Ray, K.; Begum, A.; Weyhermüller, T.; Piligkos, S.; van Slageren, J.; Neese, F.; Wieghardt, K. *J. Am. Chem. Soc.* **2005**, *127*, 4403−4415.

Table 3. Structural Features of **1**, **2**, and Related Cobalt Dithiolene Complexes

	dimer/ monomer	apical Co−S* distance (Å)	S−Co−S* angle (deg)	mean deviation of S atoms from S_4 plane (Å)[a]	deviation of Co atom from S_4 plane (Å)[b]	magnetic property
$(^nBu_4N)_2[Co(chdt)_2]_2$ (**1**)	dimer	2.348	90.9	0.12	0.25	triplet
$(^nBu_4N)_2[Co(dmdt)_2]_2$ (**2**)	dimer	2.327	85.6	0.24	0.26	diamag
$(^nBu_4N)_2[Co(dddt)_2]_2$	dimer	2.328	90.4	0.19	0.30	diamag
$(^nBu_4N)_2[Co(tcdt)_2]_2$	dimer	2.404	95.2	0.14	0.26	diamag
$(Ph_3MeAs)[Co(tdt)_2]$	monomer			0.08	0.01	triplet
$(^nBu_4N)[Co(^tBu_2bdt)_2]$	monomer			0	0	triplet

[a] Average of distances of the sulfur atoms from the best plane through four sulfur atoms around cobalt atom in a monomer unit. [b] Distances of the cobalt atom from the best plane through four sulfur atoms around cobalt atom.

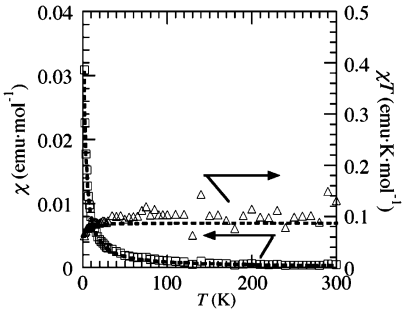

Figure 8. Temperature dependence of magnetic susceptibilities (χ) of randomly oriented polycrystals of **3** under 5 kOe. The dotted lines correspond to the Curie−Weiss plot, where the Curie constant and Weiss temperature are 8.7×10^{-2} K·emu·mol^{-1} and −0.85 K, respectively.

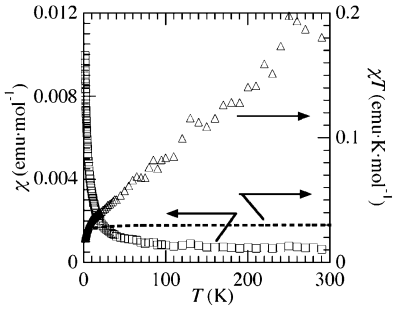

Figure 9. Temperature dependence of magnetic susceptibilities (χ) of randomly oriented polycrystals of **4** under 5 kOe. The dotted lines correspond to the magnetic behavior of the paramagnetic system with 1.6% of $S = {}^3/_2$ localized spin per molecule.

tion was 1.53×10^{-4} emu·mol^{-1} for the $(^nBu_4N)_2[Co(dmdt)_2]_2$ formula unit. In contrast to the case of **1**, only a small spin moment was observed for the measurement of **2** despite the similarity in their oxidation states. The Curie constant of **2** was almost zero ($C = 4.9 \times 10^{-3}$ K·emu·mol^{-1}) per formula unit, which suggests that all the spins are paired. To elucidate these differences in magnetic properties of **1** and **2**, we summarized several features of the crystal structures of **1**, **2**, and the reported Co dithiolene complexes that have oxidation states similar to **1** and **2**, $(^nBu_4N)_2[Co(tcdt)_2]_2$,[39] $(Ph_3MeAs)[Co(tdt)_2]$,[37] and $(^nBu_4N)[Co(^tBu_2bdt)_2]$[38], where tcdt = 3,4,5,6-tetrachlorobenzene-1,2-dithiolate and tdt = toluene-1,2-dithiolate in Table 3. The monomeric complexes, $(Ph_3MeAs)[Co(tdt)_2]$ and $(^nBu_4N)[Co(^tBu_2bdt)_2]$, have highly planar structures around the cobalt atom and exhibit paramagnetic spin triplet states, as mentioned above. On the other hand, the dimer complexes, **2** and $(^nBu_4N)_2[Co(tcdt)_2]_2$, have heavily distorted structures as judged from the large S−Co−S* angles (85.6° and 95.2°) and large mean deviations of the sulfur atoms from the S_4 plane (0.24 and 0.14 Å). Such a distortion of the ligand parts around the cobalt atom may cause a mixing of the unpaired $2b_{2g}$ and $2b_{3g}$ orbitals of the monomer units and the resultant splitting of the energy levels between these two orbitals, thereby giving rise to a spin-paired arrangement and a diamagnetic state, even in each monomer unit. In the case of **1**, the S−Co−S* angle (90.9°) is almost 90°, and the mean deviation of the sulfur atoms from the S_4 plane (0.12 Å) is much smaller than those of the above-mentioned dimers. Therefore, each monomer unit has a relatively planar structure, and complex **1** will maintain the spin-triplet state even in the dimer form.

Table 4. Overlap Integrals ($\times 10^{-3}$) of **4**

[a]	HOMO− HOMO	LUMO− LUMO	HOMO− LUMO	LUMO− HOMO
A1	−5.93	3.70	5.01	−5.01
P1	−0.61	1.04	0.80	−0.80
D1	3.62	−1.43	2.32	−2.32
R1	2.61	−4.12	3.28	−3.28
C1	4.19	1.82	2.08	−2.08

[a] The relation of the molecular arrangement are given in Figure 4.

Unlike the case of **2**, **3** exhibited a temperature dependence of susceptibility which could be well-fitted by a Curie−Weiss plot (Figure 8). The room-temperature susceptibility of **3** is 9.8×10^{-4} emu·mol^{-1}. The Curie constant ($C = 8.7 \times 10^{-2}$ K·emu·mol^{-1}) corresponds to 23% of the $S = {}^1/_2$ (or 4.6% of $S = {}^3/_2$) spin moment per formula unit, and the Weiss temperature ($\theta = -0.85$ K) indicates a very slight antiferromagnetic interaction. The origin of the small magnetic moment is not clear at present.

On the other hand, the magnetic susceptibility of the polycrystalline sample of **4** was also measured at 5 kOe in the temperature range of 1.9−300 K using a SQUID magnetometer. The room-temperature susceptibility of **4** was 3.5×10^{-4} emu·mol^{-1}, suggesting that the magnetic contribution from the cobalt spin is absent or very small. As shown in Figure 9, the polycrystalline sample of **4** shows almost constant magnetic susceptibilities in the temperature range of 50−300 K, suggesting a Pauli paramagnetism, and below ca. 50 K the susceptibility increases as the temperature decreases. This result is consistent with the high conductivity of **4** and indicates that **4** will be metallic down to low

(39) (a) Baker-Hawkes, M. J.; Dori, Z.; Eisenberg, R.; Gray, H. B. *J. Am. Chem. Soc.* **1968**, *90*, 4253−4259. (b) Baker-Hawkes, M. J.; Billig, E.; Gray, H. B. *J. Am. Chem. Soc.* **1966**, *88*, 4870−4875.

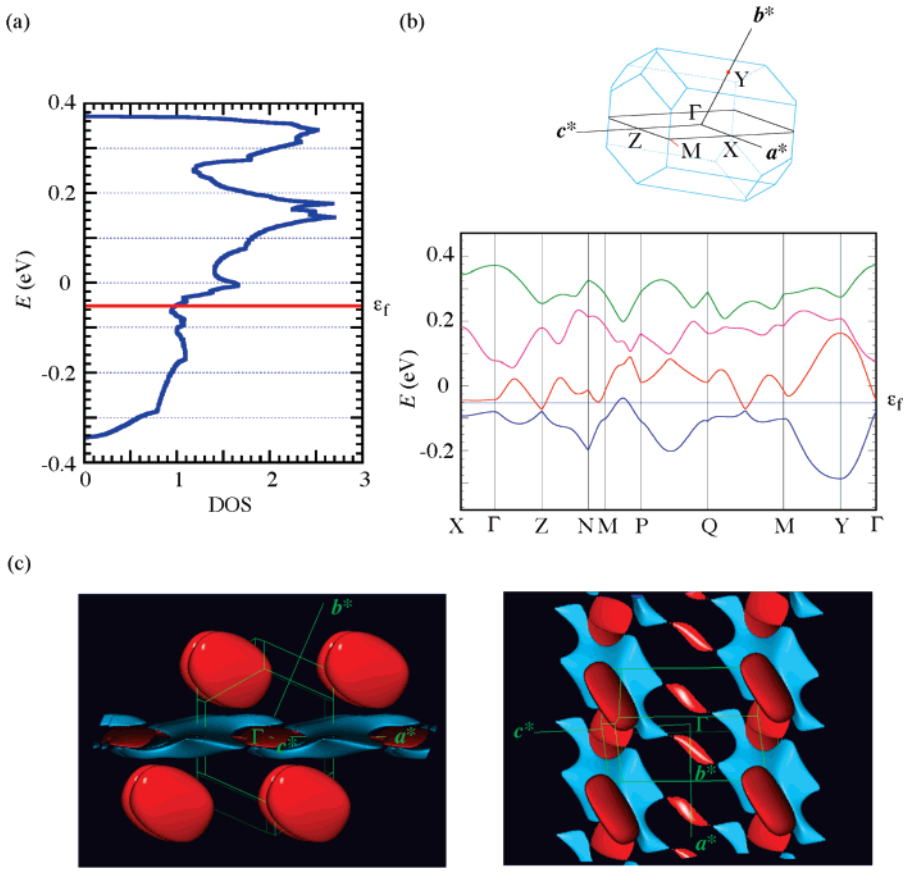

Figure 10. Band structure calculation of **4**. (a) Band energies calculated based on the obtained crystal structure of **4**. (b) DOS of **4**. (c) Calculated Fermi surfaces of **4**. Red and blue Fermi surfaces denote the electron and hole Fermi surfaces, respectively.

temperatures. The increase of magnetic susceptibilities in the low-temperature region may be due to the paramagnetic impurities and/or localized conducting electrons accrued from the lattice defect. If the magnetic behavior at low temperatures is attributed to the contribution from the cobalt spins with the $S = {}^3/_2$ high-spin state, 1.6% of the localized spins per molecule are considered to remain in complex **4**. These results imply that the difference in the oxidation states and molecular structures of the complexes determines the spin states of the monomer unit of the dimerized molecules **1**−**4**, which have large or very small magnetic moments in the anionic and neutral states.[40]

Band Structure Calculation of Neutral 4. The extended Hückel molecular orbital calculation of **3** resulted in unreasonably distorted frontier orbitals (HOMO and LUMO) probably due to the distorted dimer structure. However, more reasonable (or reliable) orbitals were obtained for **4**. Therefore, the band structure of **4** was calculated by the tight-binding method based on the extended Hückel approximation. Slater-type atomic orbitals were used to calculate the molecular orbitals. The exponents (ζ) and the ionization potentials (E_i) for the atomic orbitals are summarized in Table 2. The overlap integrals calculated on the basis of the crystal structure are also shown in Table 4. Sizable intermolecular overlap integrals along the [001] direction (the stacking direction of the $[Co(dt)_2]_2$ molecule) (C1, see Figure 4 and Table 4) were calculated for the HOMO−HOMO (4.19×10^{-3}), LUMO−LUMO (1.82×10^{-3}), HOMO−LUMO (2.08×10^{-3}), and LUMO−HOMO (-2.08×10^{-3}) interactions. On the other hand, similar large overlap integrals were also observed between the molecules of the adjacent stackings, along the [100] direction (A1), the $[\bar{1}\bar{1}0]$ direction (D1), and the $[\bar{1}11]$ direction (R1), indicating the 3D character of this complex, as shown in Table 3. The density of states (DOS) and energy dispersion curves derived from the HOMO and LUMO orbitals of $[Co(dt)_2]$ are shown in Figure 10a,b. The HOMO and LUMO bands that are formed by the HOMO and LUMO orbitals, respectively, mix with each other around the Fermi energy level (ϵ_f) and show the crossing band character of the electronic structure of this complex. The calculated Fermi surfaces are shown in Figure 10c. There are two types of electron Fermi surfaces and one type of hole Fermi surface; this indicates that **4** is a 3D metal. This result is consistent with the conducting and magnetic behaviors of **4**, thereby suggesting an essentially metallic behavior down to low temperatures.

Conclusions

We succeeded in the syntheses of novel cobalt complexes with TTF-type dithiolate ligands **1**, **2**, neutral **3**, and **4** and examined their crystal structures and physical properties. The molecular structures of these complexes were unique and

(40) According to the molecular orbital calculation based on the extended Hückel approximation, the energy gap of the HOMO and LUMO of **1** (0.00824 eV) is much smaller than that of **2** (0.01136 eV). This calculation shows that the triplet state of **1** seems to be more stable than that of **2**.

revealed that two monomeric [Co(ligand)$_2$] units have two interunit Co−S bonds and form the dimeric [Co(ligand)$_2$]$_2$ molecules. The X-ray single-crystal structure analysis of **1** showed that a short S···S contact exists between the neighboring [Co(chdt)$_2$]$_2^{2-}$ anions despite the alternating arrangement of the [Co(chdt)$_2$]$_2^{2-}$ anion and the bulky tetra-*n*-butylammonium cation. Furthermore, **1** exhibits a Curie−Weiss behavior of magnetic susceptibilities with a relatively large Curie constant and a short-range antiferromagnetic interaction ($C = 2.02$ K·emu·mol^{-1} and $\theta = -8.3$ K) in the temperature range of 1.9−300 K, thereby suggesting the existence of a spin-triplet state. Complex **2** also has an cation−anion-intermingled structure. However, the dimeric [Co(dmdt)$_2$]$_2^{2-}$ anions are completely isolated by the bulky cations; thus, there is no short S···S contact. In contrast to the case in complex **1**, the Curie constant of **2** is almost zero ($C = 4.9 \times 10^{-3}$ K·emu·mol^{-1}), suggesting that all the spins may have been cancelled by the spin-pairing that was caused by the heavy structural distortion in the [Co(dmdt)$_2$] units. On the other hand, the crystal structure analysis of **3** revealed that neutral molecules form 2D molecular stacking layers where the molecules are weakly connected to each other by S···S networks. Complex **3** shows a room-temperature conductivity (σ_{rt}) of 1.2×10^{-2} S·cm^{-1} and an activation energy (E_a) of 85 meV in the direction of the side-by-side molecular contact. The magnetic behavior is almost fitted by the Curie−Weiss law; however, the Curie constant is 8.7×10^{-2} K·emu·mol^{-1} and the Weiss temperature is estimated as −0.85 K. Furthermore, the structure determination of **4** using a powder sample revealed a uniform stacking structure of the [Co(dt)$_2$]$_2$ molecules and a 2D S···S network formed in the plane perpendicular to the stacking direction of the [Co(dt)$_2$]$_2$ molecules. The compressed pellet sample of **4** exhibited a large room-temperature electrical conductivity of 19 S·cm^{-1} and an extremely small temperature dependence ($\sigma_{0.55K}/\sigma_{rt}$ = ca. 1:10). Furthermore, the paramagnetic susceptibility of **4** was almost constant in the temperature range of 50−300 K, thereby indicating a Pauli paramagnetism in the system ($\chi_{300\ K} = 3.5 \times 10^{-4}$ emu·mol^{-1}). The relatively strong intermolecular interactions of the neutral complex [Co(dt)$_2$]$_2$ in the diagonal and side-by-side directions, which were comparable to the interaction along the stacking direction, resulted in tight-binding band structure with quasi-3D Fermi surfaces, suggesting that [Co(dt)$_2$] was a metal. Complex **4** will be a unique molecular metal that consists of a single-component molecule with a dimeric structure.

Acknowledgment. This work is financially supported by Grant-in-Aid for Scientific Research (S) (No. 14103005) and for the 21st Century COE Program for Frontiers in Fundamental Chemistry and Support of Young Researchers with a Term from the Special Coordination Fund for Promoting Science and Technology from the Ministry of Education, Culture, Sports, Science and Technology. This work is also supported by CREST (Core Research for Evolutional Science and Technology of JST (Japan Science and Technology Agency)). The authors are grateful to Prof. Y. Misaki of Ehime University for his suggestions and discussions on the synthetic method of 4,5-bis(2′-cyanoethylthio)-4,5-tetramethylene-TTF. The synchrotron radiation experiments were performed at the BL02B2 in the SPring-8 facility with the approval of the Japan Synchrotron Radiation Research Institute (JASRI) (Proposal No. 2002B0133-ND1-np).

Supporting Information Available: Four X-ray crystallographic files, in CIF format. This material is available free of charge via the Internet at http://pubs.acs.org.

IC701100R